IEEE Access
Multidisciplinary ⋮ Rapid Review ⋮ Open Access Journal

Received 26 September 2023, accepted 7 October 2023, date of publication 10 October 2023, date of current version 18 October 2023.

Digital Object Identifier 10.1109/ACCESS.2023.3323526

RESEARCH ARTICLE

Day-Ahead Forecast of Photovoltaic Power Based on a Novel Stacking Ensemble Method

LUYAO LIU[1,2], QIE SUN[3], RONALD WENNERSTEN[3], AND ZHIGANG CHEN[1]
[1]China Energy Engineering Group Guangdong Electric Power Design Institute Company Ltd., Guangzhou, Guangdong 510700, China
[2]Shenzhen International Graduate School, Tsinghua University, Shenzhen, Guangdong 518055, China
[3]Institute for Advanced Science and Technology, Shandong University, Jinan, Shandong 250061, China

Corresponding author: Luyao Liu (liuluyao@tsinghua.edu.cn)

This work was supported by the Postdoctoral Research Project of Guangdong Electric Power Design Institute under Grant EV10961W.

ABSTRACT Accurate prediction of photovoltaic (PV) power is the prerequisite for the safe and stable operation of the power grid with high penetration of PV. Despite various machine learning models for forecasting PV power have been developed, their accuracies are generally unstable. Toward this end, this study proposes a novel Stacking ensemble forecast model to improve the precision of day-ahead PV power forecasts. Different from the traditional Stacking model that uses the original training dataset to train the base learners, the proposed model creates multiple sub-training sets from the original training dataset to train the base learners, so as to enhance the diversity of base models and further improve the prediction accuracy. Specifically, in the proposed Stacking ensemble model, four machine learning learners, i.e., generalized regression neural network (GRNN), extreme learning machine (ELM), Elman neural network (ElmanNN), and Long shot-term memory (LSTM) neural network are incorporated, which are trained with the diverse sub-training datasets, and a variety of candidate base models are generated. For those candidate base models, the ones with the best performance are selected and integrated through a meta-model, namely the back-propagation network work (BPNN), to produce the final PV power prediction. The proposed model is evaluated using measured data from a 15kW PV power station in Ashland, Oregon, USA. Results indicate that across three weather scenarios, the performance of the novel Stacking ensemble model consistently outperforms single models and the traditional Stacking ensemble model in terms of the errors for out-of-sample forecasting, which proves the effectiveness of the developed procedure in improving PV power forecasting accuracy.

INDEX TERMS PV power forecast, day-ahead forecast, ensemble forecast, stacking forecast.

I. INTRODUCTION

Against the backdrop of global climate change and energy supply security, vigorously developing renewable energy has already become common targets and strategic choices for all nations. The increased manufacturing technology of photovoltaic (PV) as well as the decreased levelized costs of electricity has accelerated the development of solar power generation worldwide. In 2022, the newly installed PV capacity was 191 GW, implying a 27% growth compared to that in 2021 [1]. However, influenced by solar radiation and other meteorological factors, PV power exhibits intermittent and uncontrollable characteristics, which brings challenges to the operation stability and power quality of the power grid with high PV power integration [2]. Accurate forecasting of PV power is one of the effective measures of circumventing these adverse effects on power grid and facilitating the better utilization of solar energy.

For the PV power forecast, two main categories of methods, i.e. physical modeling [3] and data analysis [4] are adopted in the literature. The physical modelling is conducted based upon the physics theory of PV effect. In this process, atmospheric parameters, such as solar radiation, temperature, and cloud cover are first obtained from the numerical weather predictions. Subsequently, by combining these parameters with PV system installation angle and array conversion efficiency, the power generation of the PV system is calculated through physical equations [5]. Holland et al. [6] obtained the

The associate editor coordinating the review of this manuscript and approving it for publication was Fabio Mottola.

solar irradiance through the radiation transfer equations first, and then combined the forecasted solar irradiance with the PV module operation equations to estimate the future PV power. Mayer et al. [7] developed a physical model consisting of the beam and diffuse separation, tilted irradiance transposition, reflection loss, cell temperature and module performance modelling to forecast the day-ahead and intraday PV power. The downside of the physical modeling is it involves numerous parameters that are sensitive to environment, making the process cumbersome and prediction accuracy poor.

In contrast, the data analysis method make predictions by analyzing the relationship between the PV power and its historical data, as well as the meteorological factors. As PV power is a nonlinear, time-varying and multivariable coupling process, the statistical methods have restrictions and limitations for modelling this process. Machine Learning (ML) methods, e.g. Artificial Neural Network (ANN) and Deep Learning (DL) have been widely applied in this field due to their strong nonlinear mapping capabilities [8], [9]. Researchers have improved the accuracy of PV power prediction by optimizing training algorithms and structural parameters of ML models. For example, Boriratrit et al. [10] proposed developments of Extreme Learning Machine (ELM) to improve the forecasting performance of solar irradiance time series datasets, where ELM was optimized by a golden eagle optimization and a logistic map for solving overfitting and outlier sensitivity. Zhou et al. [11] reported a stochastic configuration network (SCN) for PV power prediction, which guarantees its universal approximation properties by generating stochastic parameters in different ranges based on innovative supervisory mechanisms. In another study [12], a day-ahead PV power prediction based on a Long Short-Term Memory Recurrent Neural Network (LSTM-RNN) model is proposed. This model considers the time correlation in data sequences, providing advantages over traditional ML models. Numerous ML based models have been extensively studied in the literature, and for a detailed overview of other current ML models, one can refer to specific references [13], [14], [15], [16]. Overall, ML methods offer improved accuracy in PV power prediction by effectively capturing the complex relationships between various factors. These models have been continuously refined and optimized, contributing to advancements in PV power forecasting.

However, it is important to note that no single ML model has an absolute advantage or universal adaptability [17]. As a result, ensemble forecast (EF) [18], [19] methods have become a popular approach as they can mitigate the risk of single model selection and enhance the reliability of prediction results. Ensemble forecasting involves training multiple base models and combining their outputs in a specific manner to improve prediction accuracy and stability [20], [21]. Various ensemble methods, such as Bagging, Boosting, and Stacking, have shown promising results [22], [23], [24]. Bagging and Boosting algorithms improve accuracy by aggregating the predictions of diverse base learners through simply voting or averaging [25], [26], [27]. On the contrary, Stacking algorithm utilizes meta-learners to combine the learning patterns of different base learners. Research has highlighted the importance of diversity in constructing effective ensemble forecasting models [28]. Stacking algorithm leverages the structural heterogeneity among different ML learners to generate diversity in the ensemble model. By harnessing the strengths of various base learners, better accuracy and generalization capabilities can be achieved [29].

Several studies have shown that ensemble methods using the Stacking algorithm outperform single methods in PV power forecasting performance. For instance, Jnr et al. [30] proposed a PV power forecast model using the Stacking algorithm, which employed the group method of data handling (GMDH), least squares support vector machine (LSSVM), emotional neural network (ENN), and radial basis function neural network (RBFNN) as base models, and the backpropagation neural network (BPNN) as the meta-model. This method outperformed four individual advanced methods, demonstrating its superiority in PV power forecasting. Similarly, Khan et al. [31] developed a Stacking method for day-ahead PV power prediction. This model utilized ANN and LSTM as the base models and extreme gradient boosting algorithm as the meta-learner to integrate the predictions from each base model. The proposed model showed a significant improvement in the R^2 value, ranging from 10% to 12%, compared to individual models. It also demonstrated the best combination of consistency and stability across different case studies, regardless of weather variations. However, traditional Stacking methods typically use an initial training set to train multiple base learners. This method have limitations in enhancing the diversification of base models, since they haven't considered the data discrepancies in the sub-training set, which hinders the further improvement of accuracy and reliability of PV power forecasting. To address this limitation and improve PV power forecasting performance, it is necessary to further analyze and explore new Stacking ensemble learning mechanisms.

In this paper, we propose a novel Stacking ensemble method that enhances the diversity of base models by adopting data and structure diversity enhancement techniques. This method utilizes a subsampling strategy to generate multiple sub-training sets, thereby enhancing the diversification of the data. Four sophisticated machine learning models, namely the generalized regression neural network (GRNN), ELM, Elman neural network (ElmanNN), and LSTM are considered as the base learners. By training these multiple learners with the multiple sub-training datasets, various candidate base models are generated. The base models with higher performance are filtered and integrated using the Stacking strategy through a meta-model, specifically the back-propagation neural network (BPNN), to produce the final prediction of PV power. To evaluate the proposed method, measured data from

a 15kW PV power station in Ashland, Oregon, USA, is used for simulation. By comparing the performance of the proposed method with the traditional Stacking method and individual machine learning models, the improvements in PV power forecasting accuracy and reliability are assessed.

The remainder of this paper is structured as follows: Section II provides detailed information on the methods employed in this study. Section III describes the adopted datasets and the data processing process. Section IV presents the results and discusses their implications. Finally, Section V summarizes the paper and provides concluding remarks.

II. METHODS

In this section, the proposed novel Stacking ensemble method based on data and structure diversity enhancement, and the evaluation indicators for day-ahead PV power predictions are illustrated.

A. THE NOVEL STACKING ENSEMBLE MODEL BASED ON STRUCTURE AND DATA DIVERSITY ENHANCEMENT TECHNIQUES

The proposed Stacking ensemble method aims to improve the prediction accuracy of PV power by adopting structure and data diversity enhancement techniques. The structure diversity means the heterogeneous structures of the base learners, while the data diversity refers to creating multiple sub-training sets from the initial training set.

Four distinct machine learning models, namely the GRNN, ELM, ElmanNN, and LSTM, are chosen as the base learners due to their unique structures and advantages. GRNN has a simple structure consisting of one hidden layer and one output layer. The connection weights between the hidden layer and output layer are fixed and do not require training. GRNN uses Gaussian radial basis functions to construct the activation function of the hidden layer, so as to realize the feature mapping of input data. The only parameter that needs adjustment in GRNN is the smoothing factor, which minimizes the interference of manual operation on the prediction results [32]. ELM is single-hidden layer feedforward neural network. The connection weights as well as the threshold between the input hidden layers are randomly initialized and do not require adjustment during the training process. ELM can achieve an optimum solution by adjusting the number of hidden layer neurons. This characteristic enables ELM to train with fast speed and exhibit good generalization performance [33]. ElmanNN exhibits a connection pattern similar to a feedforward network. Besides, it incorporates an internal feedback structure known as the receiving layer within the hidden layer. The receiving layer temporarily stores the output of the hidden layer, which is then delayed and fed back into the input of the hidden layer. This feedback mechanism enables the ElmanNN to capture and utilize historical state data, allowing for dynamic modeling and capturing the time-varying characteristics of the prediction process [34]. LSTM is a variant of the RNN. It introduces the cell memory units and gating mechanisms, including forgetting gates, input gates, and output gates, in the structure, which enables LSTM to retain and selectively update information over time, allowing for improved gradient flow and alleviating the issue of gradient vanishing in long sequences. LSTM is therefore particularly effective at handling long-term dependencies in time series datasets [12].

To combine the predictions of the base learners, a meta-learner called backpropagation neural network (BPNN) is utilized [26]. BPNN is a flexible and effective machine learning model that can integrate the outputs of the base learners and produce the final prediction of PV power.

The schematic diagram of the proposed Stacking ensemble model for PV power output is illustrated in Fig. 1. The proposed method consists of several steps, including generation of initial training datasets and test datasets, generation of multiple sub-training datasets, training of the base models using sub-training datasets, filtering of the optimal base models, generation of the meta-training dataset and training of the meta-model, test of the optimal base models, and test of the meta-model.

(1) Generation of initial training datasets and test datasets: Partition the original dataset into an initial training dataset (samples size is m), and an initial test dataset (samples size is n), denoted as TR and TE, respectively.

(2) Generation of multiple sub-training datasets: To maintain the sequential characteristic of the PV power time series data, random sampling is not suitable for creating the sub-training datasets, as it would disrupt the data order. Instead, this study randomly extracts several consecutive PV power time series data from the initial training dataset to create the multiple sub-training datasets, each with a sample size of s. Considering the balance of data diversity and computing load, here we set the number of the sub-training datasets as 4. These sub-training datasets are denoted as STR-A, STR-B, STR-C, STR-D. Their corresponding inputs are recorded as STRin-A, STRin-B, STRin-C, STRin-D, and the output labels of the real PV power are recorded as STRl-A, STRl-B, STRl-C, STRl-D.

(3) Training of the base models using sub-training datasets: Eeah sub-training dataset is used to train the four machine learning leaners (GRNN, ELM, ElmanNN, and LSTM). This results in a total of 16 diverse base models. The optimized hyper-parameters of each base model are determined through inner cross-validations on the corresponding sub-training dataset.

(4) Filtering of the optimal base models: Use the 16 trained base models to fit the corresponding sub-training dataset and obtain the training errors. Then, compare the overall training errors levels of GRNN, ELM, ElmanNN, and LSTM on different sub-training datasets, and pick out the sub-training dataset that yields the overall lowest training errors of the 4 machine learning learners. Record the filtered sub-training dataset as STR-X. Then, based on STR-X among the 4 base models, filter the 2 base models with lower training errors as the optimal base models (denoted as Model X1, Model X2).

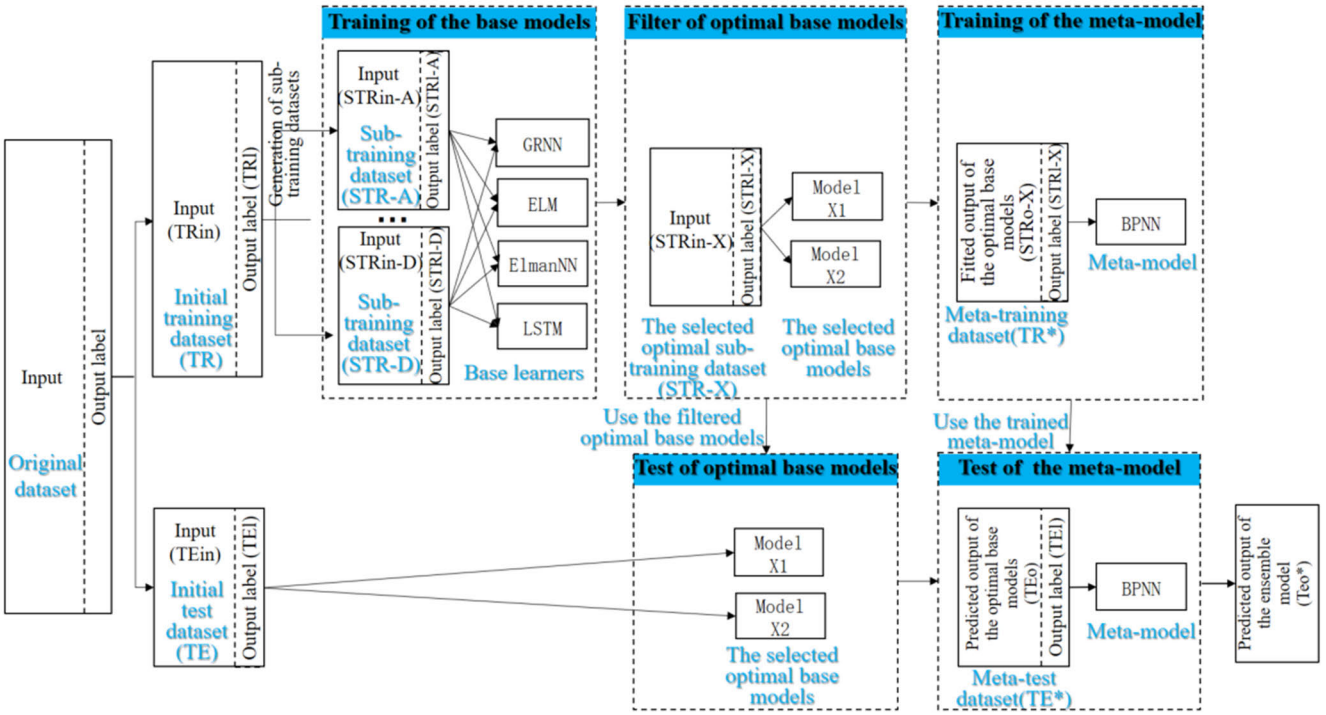

FIGURE 1. Diagram of the proposed novel Stacking ensemble forecast model.

(5) Generation of the meta-training dataset and training of the meta-model: Merge the fitting outputs of Model X1 and Model X2 (both samples size are s) horizontally to create the inputs of the meta-training dataset, and record it as STRo-X. Combine STRo-X with the output labels of real PV power at the corresponding time (STRl-X), to form the meta-training dataset (samples size is also s), and record it as TR*. Train the meta-model BPNN using TR*, and use the cross-validation method to determine the best hyper-parameters of the meta-model.

(6) Test of the optimal base models: Take the optimal base models, Model X1 and Model X2, to predict on the initial test dataset TE, and record the predicted output as TEo (samples size is m).

(7) Test of the meta-model: Combine TEo and real PV power at the corresponding time (TEl) as the meta-test dateset (TE*). Use the trained meta-model BPNN in step (5) to predict on the meta-test set TE*, and record the predicted output as TEo*. Compare TEo* with the real PV power output data to calculate the generalization error of the proposed model.

B. EVALUATION INDICATORS FOR PREDICTION ACCURACY

To quantitatively assess the performance of the proposed Stacking ensemble forecast model, three evaluation indicators are used.

(1) The Mean Absolute Percentage Error (MAPE) represents the relative deviation between predicted values and true values, also known as the average relative error.

$$\text{MAPE} = \frac{1}{N}\sum_{i=1}^{N}\left|\frac{P_{f,t}-P_{m,t}}{P_{cap}}\right|\times 100\% \tag{1}$$

where $P_{f,t}$ is the predicted value of PV power output at time t. $P_{m,t}$ is the rated output of PV power at time t. N is the number of samples in the dataset.

(2) The Mean absolute error (MAE) is an indicator to compare the absolute deviation between the predicted value and the true value.

$$\text{MAE} = \frac{1}{N}\sum_{i=1}^{N}\left|P_{f,t}-P_{m,t}\right| \tag{2}$$

(3) The Root Mean Squared Error (RMSE) is used to measure the degree of dispersion of the deviation between the predicted value and the true value.

$$\text{RMSE} = \sqrt{\text{MSE}} = \sqrt{\frac{1}{N}\sum_{i=1}^{N}\left(P_{f,t}-P_{m,t}\right)^2} \tag{3}$$

III. DATA PROCESSING

In this section, the data source, data classification and feature selection are introduced.

A. DATA SOURCE OF PV POWER AND METEROLOGICAL FACTORS

The PV power output data used in this study is from a 15 kW PV power plant located in Ashland, Oregon, USA (with an altitude of 680m, latitude of 42.19 °N, and longitude of 122.70 °W) [35]. The corresponding meteorological data

TABLE 1. Descriptive statistics of the original dataset.

		Average value	Standard deviation	Minimum value	Maximum value
Sunny	PV power output (W)	3309.05	4863.59	0.00	14690.00
	GHI (W/m^2)	284.77	366.22	0.00	1089.00
	Air temperature (℃)	16.17	9.45	-14.80	38.40
Cloudy	PV power output (W)	2538.31	4284.83	0.00	14560.00
	GHI (W/m^2)	227.01	329.03	0.00	1242.00
	Air temperature (℃)	12.52	9.56	-15.60	38.90
Rainy	PV power output (W)	1137.13	2564.27	0.00	14730.00
	GHI (W/m^2)	111.44	202.82	0.00	1317.00
	Air temperature (℃)	7.94	6.08	-11.40	34.80

of global horizontal irradiance (GHI) and air temperature is collected from [36]. The data used in this study ranges from January 1, 2018 to December 31, 2019, with a data resolution of 15 minutes. The descriptive statistics of the original dataset is given in Table 1.

B. WEATHER CLASSIFICATION BASED ON RADIATION INDEX

Weather classification is an effective preprocessing step to improve the short-term prediction accuracy of PV power [37]. Various criteria can be used for weather classification, such as radiation intensity and cloud type. In this study, the radiation index k_d is employed, which represents the ratio of Diffuse Horizontal Irradiance (DHI) to Global Horizontal Irradiance (GHI) [38]. The dataset is categorized into three types: Type 1 (sunny), Type 2 (cloudy), and Type 3 (rainy), as presented in Table 2. The number of data samples for sunny, cloudy, and rainy days is 22464, 19872, and 27744, respectively, corresponding to 234, 207, and 289 days. Fig. 2 illustrates the typical PV power output curves for the three weather conditions.

TABLE 2. Weather classification of the dataset according to k_d.

Dataset type	Weather condition	Range of k_d
Type 1	Sunny	k_d<0.15
Type 2	Cloudy	0.15≤ k_d <0.45
Type 3	Rainy	k_d ≥0.45

C. FEATURE SELECTION

To predict the PV power output P_d^t at time t on day d one day in advance, two types of candidate input features are considered. One is the historical power output, referring to the PV power output at the same time from the last day to previous seven days, denoted as P_{d-1}^t, P_{d-2}^t, …, P_{d-7}^t. The other type is the meteorological factors, including the total global horizontal irradiance G_d^t and the predicted temperature T_d^t. Using the Pearson correlation coefficient method, the correlation test between each candidate input feature and the PV power based on each sub-training dataset is conducted. The candidate inputs with a correlation coefficient greater than 0.4 (underlined) under three weather conditions are considered as the optimal input features, as shown in Table 3.

TABLE 3. The pearson correlation test and the selected optimal input features.

Data type	Sub-training dataset	P_t^{d-1}	P_t^{d-2}	P_t^{d-3}	P_t^{d-4}	P_t^{d-5}	P_t^{d-6}	P_t^{d-7}	G_t^d	T_t^d
Sunny	STR-A	**0.95**	**0.90**	**0.85**	**0.83**	**0.82**	**0.81**	**0.78**	**0.82**	0.39
	STR-B	**0.99**	**0.99**	**0.99**	**0.98**	**0.96**	**0.95**	**0.95**	**0.97**	0.39
	STR-C	**0.82**	0.46	**0.87**	**0.85**	**0.93**	**0.91**	**0.89**	**0.88**	**0.86**
	STR-D	**0.84**	0.37	**0.76**	**0.92**	**0.88**	**0.85**	**0.81**	**0.78**	**0.74**
Cloudy	STR-A	**0.90**	**0.85**	**0.82**	**0.78**	**0.75**	**0.71**	**0.68**	**0.70**	0.30
	STR-B	**0.90**	**0.86**	**0.82**	**0.79**	**0.77**	**0.75**	**0.71**	**0.95**	0.27
	STR-C	**0.66**	0.20	**0.89**	**0.84**	**0.79**	**0.71**	**0.65**	0.58	0.51
	STR-D	**0.79**	0.37	**0.90**	**0.75**	**0.68**	**0.69**	**0.63**	**0.67**	0.50
Rainy	STR-A	**0.58**	0.21	-0.09	-0.13	-0.09	0.20	**0.59**	**0.60**	0.16
	STR-B	**0.58**	0.12	-0.17	-0.18	-0.16	0.10	**0.58**	**0.92**	0.30
	STR-C	**0.87**	0.21	**0.67**	0.05	-0.20	-0.20	-0.19	0.07	0.56
	STR-D	**0.93**	0.18	**0.78**	-0.03	-0.12	-0.12	-0.12	-0.02	0.32

IV. RESULTS

In this section, the optimized hyper-parameters of the base models, the selection of the optimal base models, and the optimized parameters of the meta-model are reported respectively. Finally, the out-of-sample forecasting performance of the ensemble forecast model is compared with single models under three weather scenarios to illustrate the effectiveness of the developed method.

A. THE OPTIMIZED HYPER-PARAMETERS OF THE BASE MODELS

For each weather type, the original dataset is divided into an initial training dataset, which consist of the first 2/3 of the original dataset, and a test dataset, which consists of the last 1/3 of the original dataset. Four sub-training datasets (STR-A, STR-B, STR-C, STR-D) are extracted from the initial training dataset. The number of samples in each sub-training dataset is 1/2 of the initial training dataset, which is 7488, 6624, and 9248 for sunny, cloudy, and rainy weather, respectively.

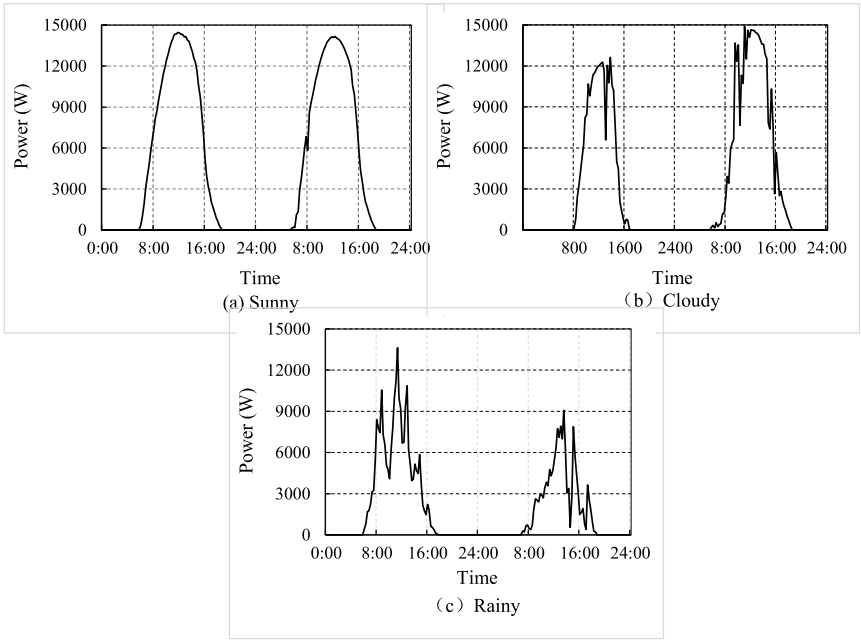

FIGURE 2. Typical PV output curves for the three weather conditions. (a) Sunny, (b) Cloudy, (c) Rainy.

TABLE 4. The start-end position in the original PV power time series data of each sub-training dataset under sunny, cloudy and rainy weather.

	STR-A	STR-B	STR-C	STR-D
Sunny	1^{st}-7488^{th}	7489^{th} -14976^{th}	2497^{th} -9984^{th}	3497^{th} -10984^{th}
Cloudy	1^{st} -6624^{th}	6625^{th} -13248^{th}	2209^{th} -8832^{nd}	3309^{th} -9832^{nd}
Rainy	1^{st} -9248^{th}	9249^{th} -18496^{th}	3083^{th} -12330^{th}	4083^{th} -13330^{th}

Note: Take the notation '1^{st}-7488^{th}' as an example to explain its meaning. The notation '1^{st}-7488^{th}' represents that the start and end positions of the sub-training dataset STR-A under sunny weather is the 1^{st} sample and the 7488^{th} sample of the original PV power time series data. The interpretations regarding other sub-training datasets follow a similar pattern to this example.

Since the sub-training datasets are chronological time series data, we use the form of 'start position-end position' in the original PV power time series data to describe each sub-training dataset. The specific start and end positions in the PV power data samples for the sub-training datasets are provided in Table 4.

According to the chosen optimal input features in Table 2, the number of the input and output layer neurons for each base model on the sub training sets STR-A, STR-B, STR-C, STR-D is {8,1},{8,1},{8,1},{8,1} under sunny weather; {8,1}, {8,1}, {6,1}, {7,1} under cloudy weather; {3,1}, {3,1}, {2,1}, {2,1} under rainy weather.

Four machine learning learners of GRNN, ELM, ElmanNN, and LSTM are trained on the four sub-training datasets, forming a total of 16 base models. Each base model is trained independently to optimize its model hyper-parameters. The hyper-parameters include activation functions, training algorithms, learning rate, etc. The available options and the adjustment range of the hyper-parameters for each base learner are provided in Table 5. To determine the optimum parameters, an initial option or value is chosen based on testing, and the best solution is obtained by iteratively adjusting the parameters within the given search space through error feedback over a certain number of iterations. The optimum hyper-parameters for the base models under sunny, cloudy, and rainy conditions are reported in Table 6.

B. THE SELECTION OF THE OPTIMAL BASE MODELS

Based on the optimized hyper-parameters, the base models (Model 1-16) are used to fit the corresponding sub-training dataset, and the resulting error is the training error. This training error reflects the fitting and generation capability of the base models on the specific sub-training dataset. Table 7 presents the training errors of Model 1-16 on their respective sub-training datasets.

For each weather condition, there exist one sub-training dataset where the four base learners exhibit the best forecasting performance compared to the other sub-training datasets. Specifically, under sunny, cloudy, and rainy weather conditions, the optimal sub-training datasets are STR-B, STR-B, and STR-B, respectively. By comparing the training effects of each base model on the STR-B dataset, the optimal base models for integration are selected and marked with '✓' in Table 7. It is important to note that the number of optimal base models should be greater than 2 since a single column of the fitting output cannot be used as the input for the meta-model. For sunny, cloudy, and rainy weather conditions, the filtered optimal models are GRNN, LSTM; GRNN, ElmanNN; and ELM, ElmanNN, respectively.

TABLE 5. The available options and adjustment range of hyper-parameters of the base learners.

Base learner	Hype-parameters	Available options/Adjustment range
GRNN	Spread value	0.01-1
ELM	Hidden layer activation function	Logistic; Hyperbolic tangent; Rectified linear unit
	Number of hidden layer neurons	2-300
ElmanNN	Hidden layer activation function	Logistic; Hyperbolic tangent; Rectified Linear Unit
	Training algorithm*	Adaptive learning rate gradient descent (Adagrad); Gradient descent with momentum (GDM); Stochastic gradient descent (SGD); Levenberg-Marquardt (LM); Adaptive moment estimation (Adam)…
	Number of hidden layers	1-2
	Number of hidden layer neurons	2-100
	Learning rate	0.01-0.3
	Iteration times	100-2000
	Iteration goal	0.00001-0.01
LSTM	Gate activation function	Logistic; Hyperbolic tangent
	Training algorithm*	Adaptive learning rate gradient descent (Adagrad); Gradient descent with momentum (GDM); Stochastic gradient descent (SGD); Levenberg-Marquardt (LM); Adaptive moment estimation (Adam)…
	Number of hidden layers	1-10
	Initial learning rate	0.01-0.3
	Learning rate schedule	None; piecewise
	Learning rate drop factor	0.1-0.5
	Learning rate drop period	10-1000
	Minimum batch size	10-500
	Maximum iteration epochs	10-1000

*Note: In addition to the aforementioned training algorithms, there are still many other training algorithms that have been developed in the field of machine learning, such as batch gradient descent, mini-batch gradient descent, conjugate gradient descent, root mean square propagation. Due to space limitations, this table only provides a selection of typical training algorithms for illustration purposes.

C. THE OPTIMIZED HYPER-PARAMETERS OF THE META-MODEL

Based on the filtered optimal base models, their fitting outputs are combined with the PV power labels at the corresponding time to form the meta-training set of the meta-model BPNN. The number of the input and output layer neurons of the meta-model is equal to the dimension of input and output of the meta-training set. According to Table 7, the number of the input layer neurons for the meta-model BPNN under sunny, cloudy, and rainy weather conditions is 2, 2, and 2, respectively, and the number of output layer neurons for the meta-model under sunny, cloudy, and rainy weather is 1, 1, and 1.

The meta-model BPNN is trained to determine its best hyper-parameters. The available options and adjustment range of the hyper-parameters for the meta-model are provided in Table 8. The optimized hyper-parameters of the meta-model under three weather scenarios are shown in Table 9.

D. COMPARISON OF THE PROPOSED NOVEL STACKING MODEL WITH SINGLE MODELS AND THE TRADITIONAL STACKING MODEL

The curve comparison between the predicted and real PV power output values based on the proposed novel Stacking ensemble forecast model on part of the test sets is shown in Fig. 3. It is observed that the predicted values are very close to the true values.

The results of the forecasting performance in terms of generalization errors on the test set predicted by the novel Stacking ensemble model, single models, and the traditional Stacking ensemble model under three weather types are shown in Fig. 4. The proposed novel Stacking ensemble forecast model demonstrates several advantages over single models and the traditional Stacking model, as illustrated in the performance comparison. Fig. 4 shows that the proposed Stacking ensemble forecast model consistently exhibits the smallest MAPE, MAE, and RMSE values across all weather scenarios, which are 2.0%, 0.302 kW, and 0.475 kW under sunny conditions, 3.6%, 0.542 kW, and 0.830 kW under cloudy conditions, 4.1%, 0.613 kW, and 1.012 kW under rainy conditions, significantly lower than those of the single GRNN model, ELM model, ElmanNN, and LSTM model. What's more, it is observed that the forecasting performance in terms of the out-of-sample errors of the traditional Stacking model slightly improves upon the individual models in sunny and rainy weather conditions, and it does not improve in cloudy weather. In contrast, the proposed Stacking ensemble model leverages the differences among the base models, through the data and structure enhancement

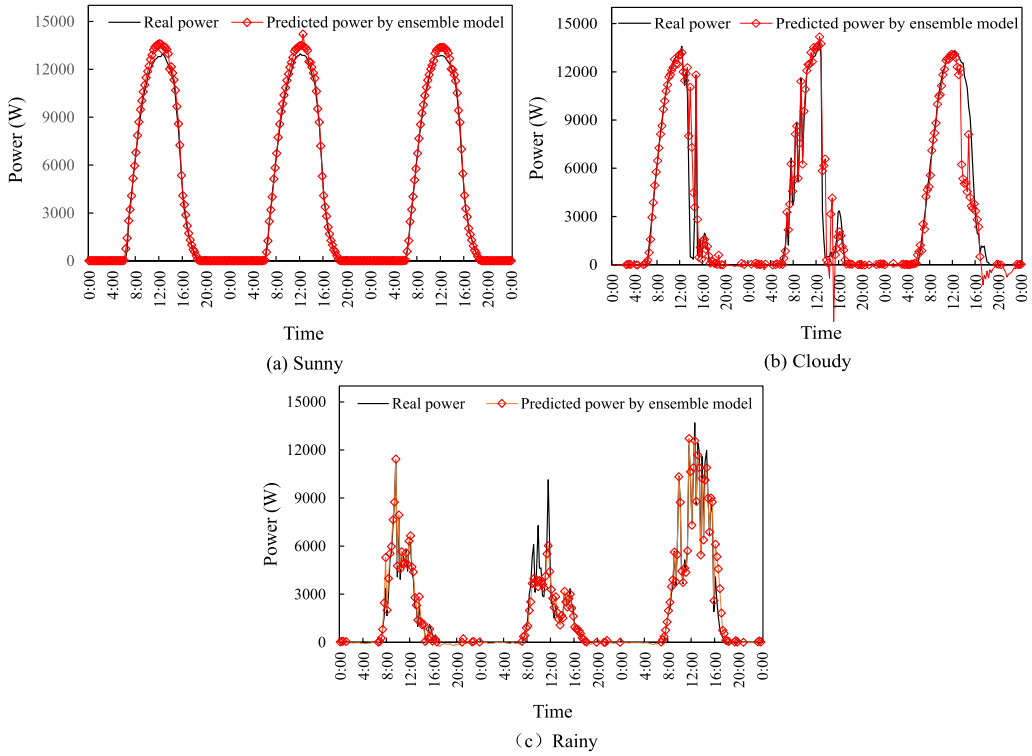

FIGURE 3. Comparison of the predicted and actual PV power output by the ensemble model based on a part of the test datasets under different weather types. (a) Sunny, (b) Cloudy, and (c) Rainy.

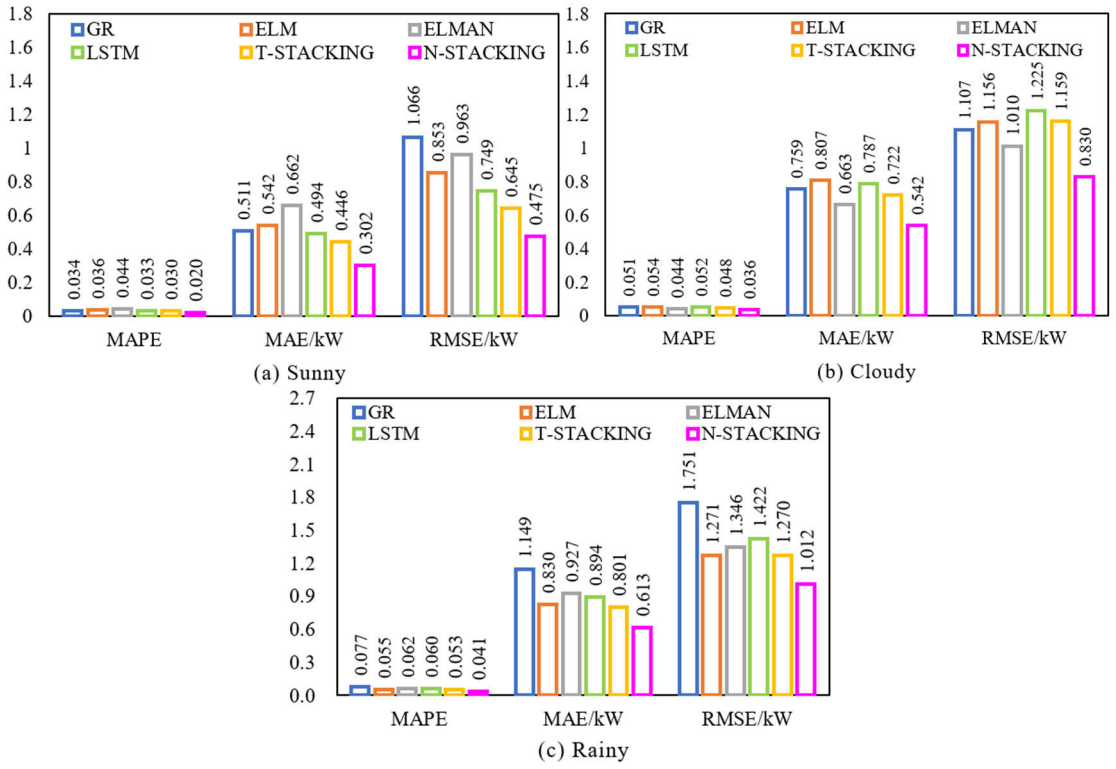

FIGURE 4. The generalization errors on the test set of the proposed Stacking ensemble forecast model, the traditional Stacking model and single models under different weather conditions. (a) Sunny, (b) Cloudy, and (c) Rainy.

TABLE 6. The optimized hyper-parameters of the trained base learners based on the corresponding sub-training dataset under sunny, cloudy, and rainy weather.

Sub-training dataset	Learner	Hype-parameters	Sunny	Cloudy	Rainy
STR-A	GRNN	Spread value	0.1	0.2	0.1
	ELM	Hidden layer activation function	Logistic	Logistic	Logistic
		Number of hidden layer neurons	10	100	100
	ElmanNN	Hidden layer activation function	Logistic	Logistic	Logistic
		Training algorithm	LM	LM	LM
		Number of hidden layers	1	1	1
		Number of hidden layer neurons	5	15	8
		Learning rate	0.1	0.2	0.3
		Iteration times	200	2000	1000
		Iteration goal	0.01	0.01	0.0001
	LSTM	Gate activation function	Logistic	Logistic	Logistic
		Training algorithm	Adam	Adam	Adam
		Number of hidden layers	5	8	4
		Initial learning rate	0.01	0.01	0.01
		Learning rate schedule	Piecewise	Piecewise	Piecewise
		Learning rate drop factor	0.1	0.2	0.5
		Learning rate drop period	100	200	200
		Minimum batch size	120	150	200
		Maximum iteration epochs	500	1600	800
STR-B	GRNN	Spread value	0.1	0.2	0.2
	ELM	Hidden layer activation function	Logistic	Logistic	Logistic
		Number of hidden layer neurons	50	10	20
	ElmanNN	Hidden layer activation function	Logistic	Logistic	Logistic
		Training algorithm	LM	LM	LM
		Number of hidden layers	1	1	1
		Number of hidden layer neurons	15	20	5
		Learning rate	0.1	0.2	0.1
		Iteration times	200	1000	2000
		Iteration goal	0.01	0.01	0.0001
	LSTM	Gate activation function	Logistic	Logistic	Logistic
		Training algorithm	Adam	Adam	Adam
		Number of hidden layers	5	4	10
		Initial learning rate	0.1	0.1	0.1
		Learning rate schedule	Piecewise	Piecewise	Piecewise
		Learning rate drop factor	0.5	0.5	0.5
		Learning rate drop period	50	100	50
		Minimum batch size	20	100	260
		Maximum iteration epochs	1200	2000	1000
STR-C	GRNN	Spread value	0.2	0.1	0.01
	ELM	Hidden layer activation function	Logistic	Logistic	Logistic
		Number of hidden layer neurons	110	90	60
	ElmanNN	Hidden layer activation function	Logistic	Logistic	Logistic
		Training algorithm	SGD	SGD	SGD
		Number of hidden layers	1	1	1
		Number of hidden layer neurons	15	5	30
		Learning rate	0.3	0.1	0.2
		Iteration times	600	1500	1000
		Iteration goal	0.001	0.01	0.0001
	LSTM	Gate activation function	Logistic	Logistic	Logistic
		Training algorithm	Adam	Adam	Adam
		Number of hidden layers	4	6	6
		Initial learning rate	0.01	0.01	0.01
		Learning rate schedule	Piecewise	Piecewise	Piecewise
		Learning rate drop factor	0.3	0.2	0.1
		Learning rate drop period	100	100	100
		Minimum batch size	200	50	100
		Maximum iteration epochs	2000	500	300
	GRNN	Spread value	0.1	0.2	0.01
	ELM	Hidden layer activation function	Logistic	Logistic	Logistic
		Number of hidden layer neurons	130	80	100
	ElmanNN	Hidden layer activation function	Logistic	Logistic	Logistic
		Training algorithm	GDM	GDM	GDM

TABLE 6. *(Continued.)* **The optimized hyper-parameters of the trained base learners based on the corresponding sub-training dataset under sunny, cloudy, and rainy weather.**

STR-D		Number of hidden layers	1	1	1
		Number of hidden layer neurons	12	25	40
		Learning rate	0.1	0.2	0.1
		Iteration times	900	1200	700
		Iteration goal	0.001	0.1	0.001
	LSTM	Gate activation function	Logistic	Logistic	Logistic
		Training algorithm	Adam	Adam	Adam
		Number of hidden layers	4	6	3
		Initial learning rate	0.1	0.1	0.1
		Learning rate schedule	Piecewise	Piecewise	Piecewise
		Learning rate drop factor	0.1	0.2	0.5
		Learning rate drop period	200	100	200
		Minimum batch size	180	300	400
		Maximum iteration epochs	2000	700	800

TABLE 7. **Training error of each base model on the corresponding sub training dataset based on the optimal hyper-parameters under different weather conditions.**

Base model number		1	2	3	4	5	6	7	8	9	10	11	12	13	14	15	16
Base learner		GRNN	ELM	Elman	LSTM	GRNN	ELM	Elman	LSTM	GRNN	ELM	Elman	LSTM	GRNN	ELM	Elman	LSTM
Sub-training dataset		**STR-A**				**STR-B**				**STR-C**				**STR-D**			
Sunny	MAPE	0.032	0.050	0.047	0.051	**0.019**	0.022	0.041	**0.017**	0.027	0.033	0.038	0.040	0.022	0.027	0.033	0.036
	MAE (kW)	0.492	0.758	0.704	0.766	**0.299**	0.332	0.623	**0.260**	0.401	0.494	0.566	0.596	0.327	0.402	0.488	0.533
	RMSE (kW)	1.341	1.612	1.522	1.815	**0.441**	0.459	0.801	**0.386**	1.061	1.138	1.347	1.405	0.997	1.023	1.185	1.222
						✓			✓								
Cloudy	MAPE	0.049	0.066	0.060	0.075	**0.025**	0.067	**0.041**	0.043	0.027	0.050	0.056	0.071	0.044	0.047	0.050	0.065
	MAE (kW)	0.746	0.994	0.908	1.129	**0.384**	1.017	**0.615**	0.651	0.400	0.753	0.835	1.060	0.659	0.712	0.754	0.981
	RMSE (kW)	1.587	1.740	1.744	1.859	**0.782**	1.408	**0.941**	0.963	1.151	1.488	1.590	1.773	1.412	1.436	1.525	1.684
						✓		✓									
Rainy	MAPE	0.052	0.069	0.068	0.063	0.050	**0.037**	**0.038**	0.042	0.054	0.057	0.064	0.055	0.066	0.055	0.061	0.056
	MAE (kW)	0.785	1.041	1.032	0.947	0.750	**0.563**	**0.576**	0.628	0.810	0.857	0.953	0.832	0.992	0.830	0.918	0.833
	RMSE (kW)	1.719	1.878	1.859	1.642	1.208	**1.049**	**1.090**	1.109	1.608	1.572	1.829	1.603	1.675	1.490	1.601	1.554
							✓	✓									

TABLE 8. **The available options and adjustment range of hyper-parameters of the meta-model.**

Hype-parameters	Available Options/Adjustment range
Hidden layer activation function	Logistic; Hyperbolic tangent; Rectified linear unit
Training algorithm*	Adaptive learning rate gradient descent (Adagrad); Gradient descent with momentum (GDM); Stochastic gradient descent (SGD); Levenberg-Marquardt (LM); Adaptive moment estimation (Adam)…
Number of hidden layers	1-2
Number of hidden layer neurons	2-100
Learning rate	0.01-0.3
Iteration times	10-1000
Iteration goal	0.00001-0.01

techniques, resulting in the strongest generalization capacity across all weather conditions.

Additionally, the generation performance of each single model under different weather circumstances is inconsistent, as observed in Fig. 4. For example, compared with the other single models, the ElmanNN model performs best under cloudy weather but is weaker under sunny weather. The LSTM model has the best performance under sunny weather but is not the best for other weather conditions. This inconsistency highlights the risk of relying on a single model for forecasting. By enhancing the diversity of base models, the proposed novel Stacking ensemble model achieves a robust performance and avoids the problems of forecasting instability caused by reliance on a single model.

The superiority of the novel Stacking model can be attributed to its inner structure and data diversity enhance-

TABLE 9. The optimized hyper-parameters of the meta-model under sunny, cloudy, and rainy weather.

Hyper-parameters	Sunny	Cloudy	Rainy
Hidden layer activation function	Logistic	Logistic	Logistic
Training algorithm	Adagrad	Adagrad	Adagrad
Number of hidden layer	1	1	1
Number of hidden layer neurons	2	3	5
Learning rate	0.1	0.01	0.1
Iteration times	200	100	100
Iteration goal	0.00004	0.00004	0.00004

ment mechanisms. The combination of multiple sub-training sets and multiple neural network learners allows for the production of multiple base models with different parameters under each weather condition, providing a multiplicity basis for the establishment of the ensemble model. The critical step of selecting the models with prime performance for integration from diverse base models and discarding the underperforming ones ensures the accuracy improvement of the ensemble forecast model.

V. CONCLUSION

This study proposes a novel Stacking ensemble method for day-ahead prediction of the PV power output, which utilizes the data and structure diversity enhancement techniques to increase the diversity among base models. This method incorporates multiple machine learning learners with different structures, namely GRNN, ELM, ElmanNN, and LSTM to ensure structure diversity. Additionally, it generates multiple sub-training sets from the initial training set to achieve data diversity. Using multiple sub-training sets to train the four heterogeneous learners, diverse candidate base models are produced and the best-performing ones are filtered and then integrated using a meta-model, i.e. BPNN to obtain the final prediction of the PV power output.

Real measured data from a 15kW PV power station in Ashland, Oregon is used to evaluate the proposed model. Results demonstrate that the proposed novel Stacking ensemble model consistently outperforms the single models as well as the traditional Stacking model in terms of MAE, MAPE, and RMSE, regardless of weather variations. This confirms the effectiveness of the proposed method in improving the generalization performance of the PV power prediction.

Overall, the proposed method leverages the strengths of the Stacking ensemble approach while introducing a novel approach to training the base learners. This enhances the diversity of the base models and ultimately improves the accuracy of PV power prediction. The proposed method enriches the theories of PV power ensemble forecast. Additionally, this method can be applied to other renewable energy forecasting tasks to evaluate its generalizability and effectiveness in different contexts. By applying this model in practice, it will contribute to promoting the stable operation and economic dispatch of power systems with high renewable energy integration.

ACKNOWLEDGMENT

The authors would like to thank the Solar Radiation Monitoring Laboratory, University of Oregon, for providing the data for this research. This work is supported by Postdoctoral Research Project of Guangdong Electric Power Design Institute (No. EV10961W).

REFERENCES

[1] *Renewables*, Int. Energy Agency, Paris, France, 2021.

[2] J. Zhu, M. Li, L. Luo, B. Zhang, M. Cui, and L. Yu, "Short-term PV power forecast methodology based on multi-scale fluctuation characteristics extraction," *Renew. Energy*, vol. 208, pp. 141–151, May 2023, doi: 10.1016/j.renene.2023.03.029.

[3] T. Ma, H. Yang, and L. Lu, "Solar photovoltaic system modeling and performance prediction," *Renew. Sustain. Energy Rev.*, vol. 36, pp. 304–315, Aug. 2014, doi: 10.1016/j.rser.2014.04.057.

[4] L. Liu, Y. Zhao, D. Chang, J. Xie, Z. Ma, Q. Sun, H. Yin, and R. Wennersten, "Prediction of short-term PV power output and uncertainty analysis," *Appl. Energy*, vol. 228, pp. 700–711, Oct. 2018, doi: 10.1016/j.apenergy.2018.06.112.

[5] M. P. Almeida, M. Muñoz, I. de la Parra, and O. Perpiñán, "Comparative study of PV power forecast using parametric and nonparametric PV models," *Sol. Energy*, vol. 155, pp. 854–866, Oct. 2017, doi: 10.1016/j.solener.2017.07.032.

[6] N. Holland, X. Pang, W. Herzberg, S. Karalus, J. Bor, and E. Lorenz, "Solar and PV forecasting for large PV power plants using numerical weather models, satellite data and ground measurements," in *Proc. IEEE 46th Photovolt. Spec. Conf. (PVSC)*, Jun. 2019, pp. 1609–1614, doi: 10.1109/PVSC40753.2019.8980496.

[7] M. J. Mayer and G. Gróf, "Extensive comparison of physical models for photovoltaic power forecasting," *Appl. Energy*, vol. 283, Feb. 2021, Art. no. 116239, doi: 10.1016/j.apenergy.2020.116239.

[8] W. VanDeventer, E. Jamei, G. S. Thirunavukkarasu, M. Seyedmahmoudian, T. K. Soon, B. Horan, S. Mekhilef, and A. Stojcevski, "Short-term PV power forecasting using hybrid GASVM technique," *Renew. Energy*, vol. 140, pp. 367–379, Sep. 2019, doi: 10.1016/j.renene.2019.02.087.

[9] T. Limouni, R. Yaagoubi, K. Bouziane, K. Guissi, and E. H. Baali, "Accurate one step and multistep forecasting of very short-term PV power using LSTM-TCN model," *Renew. Energy*, vol. 205, pp. 1010–1024, Mar. 2023, doi: 10.1016/j.renene.2023.01.118.

[10] S. Boriratrit, P. Fuangfoo, C. Srithapon, and R. Chatthaworn, "Adaptive meta-learning extreme learning machine with golden eagle optimization and logistic map for forecasting the incomplete data of solar irradiance," *Energy AI*, vol. 13, Jul. 2023, Art. no. 100243, doi: 10.1016/j.egyai.2023.100243.

[11] X. Zhou, Y. Ao, X. Wang, X. Guo, and W. Dai, "Learning with privileged information for short-term photovoltaic power forecasting using stochastic configuration network," *Inf. Sci.*, vol. 619, pp. 834–848, Jan. 2023, doi: 10.1016/j.ins.2022.11.046.

[12] F. Wang, Z. Xuan, Z. Zhen, K. Li, T. Wang, and M. Shi, "A day-ahead PV power forecasting method based on LSTM-RNN model and time correlation modification under partial daily pattern prediction framework," *Energy Convers. Manage.*, vol. 212, May 2020, Art. no. 112766, doi: 10.1016/j.enconman.2020.112766.

[13] R. Ahmed, V. Sreeram, Y. Mishra, and M. D. Arif, "A review and evaluation of the state-of-the-art in PV solar power forecasting: Techniques and optimization," *Renew. Sustain. Energy Rev.*, vol. 124, May 2020, Art. no. 109792, doi: 10.1016/j.rser.2020.109792.
[14] H. Wang, Z. Lei, X. Zhang, B. Zhou, and J. Peng, "A review of deep learning for renewable energy forecasting," *Energy Convers. Manage.*, vol. 198, Oct. 2019, Art. no. 111799, doi: 10.1016/j.enconman.2019.111799.
[15] U. K. Das, K. S. Tey, M. Seyedmahmoudian, S. Mekhilef, M. Y. I. Idris, W. Van Deventer, B. Horan, and A. Stojcevski, "Forecasting of photovoltaic power generation and model optimization: A review," *Renew. Sustain. Energy Rev.*, vol. 81, pp. 912–928, Jan. 2018, doi: 10.1016/j.rser.2017.08.017.
[16] R. Pugliese, S. Regondi, and R. Marini, "Machine learning-based approach: Global trends, research directions, and regulatory standpoints," *Data Sci. Manage.*, vol. 4, pp. 19–29, Dec. 2021, doi: 10.1016/j.dsm.2021.12.002.
[17] Z. Wang, I. Koprinska, A. Troncoso, and F. Martínez-Álvarez, "Static and dynamic ensembles of neural networks for solar power forecasting," in *Proc. Int. Joint Conf. Neural Netw. (IJCNN)*, Jul. 2018, pp. 1–8, doi: 10.1109/IJCNN.2018.8489231.
[18] Y. Ren, P. N. Suganthan, and N. Srikanth, "Ensemble methods for wind and solar power forecasting—A state-of-the-art review," *Renew. Sustain. Energy Rev.*, vol. 50, pp. 82–91, Oct. 2015, doi: 10.1016/j.rser.2015.04.081.
[19] S. Ma, "A hybrid deep meta-ensemble networks with application in electric utility industry load forecasting," *Inf. Sci.*, vol. 544, pp. 183–196, Jan. 2021, doi: 10.1016/j.ins.2020.07.054.
[20] A. Nespoli, S. Leva, M. Mussetta, and E. G. C. Ogliari, "A selective ensemble approach for accuracy improvement and computational load reduction in ANN-based PV power forecasting," *IEEE Access*, vol. 10, pp. 32900–32911, 2022, doi: 10.1109/ACCESS.2022.3158364.
[21] M. Massaoudi, H. Abu-Rub, S. S. Refaat, M. Trabelsi, I. Chihi, and F. S. Oueslati, "Enhanced deep belief network based on ensemble learning and tree-structured of Parzen estimators: An optimal photovoltaic power forecasting method," *IEEE Access*, vol. 9, pp. 150330–150344, 2021, doi: 10.1109/ACCESS.2021.3125895.
[22] S. Al-Dahidi, O. Ayadi, M. Alrbai, and J. Adeeb, "Ensemble approach of optimized artificial neural networks for solar photovoltaic power prediction," *IEEE Access*, vol. 7, pp. 81741–81758, 2019, doi: 10.1109/ACCESS.2019.2923905.
[23] G. An, Z. Jiang, X. Cao, Y. Liang, Y. Zhao, Z. Li, W. Dong, and H. Sun, "Short-term wind power prediction based on particle swarm optimization-extreme learning machine model combined with AdaBoost algorithm," *IEEE Access*, vol. 9, pp. 94040–94052, 2021, doi: 10.1109/ACCESS.2021.3093646.
[24] J. Shi, C. Li, and X. Yan, "Artificial intelligence for load forecasting: A stacking learning approach based on ensemble diversity regularization," *Energy*, vol. 262, Jan. 2023, Art. no. 125295, doi: 10.1016/j.energy.2022.125295.
[25] G. Mitrentsis and H. Lens, "An interpretable probabilistic model for short-term solar power forecasting using natural gradient boosting," *Appl. Energy*, vol. 309, Mar. 2022, Art. no. 118473, doi: 10.1016/j.apenergy.2021.118473.
[26] M. H. D. M. Ribeiro, R. G. da Silva, S. R. Moreno, V. C. Mariani, and L. D. S. Coelho, "Efficient bootstrap stacking ensemble learning model applied to wind power generation forecasting," *Int. J. Electr. Power Energy Syst.*, vol. 136, Mar. 2022, Art. no. 107712, doi: 10.1016/j.ijepes.2021.107712.
[27] M. Q. Raza, N. Mithulananthan, and A. Summerfield, "Solar output power forecast using an ensemble framework with neural predictors and Bayesian adaptive combination," *Sol. Energy*, vol. 166, pp. 226–241, May 2018, doi: 10.1016/j.solener.2018.03.066.
[28] F. Schwenker, "Ensemble methods: Foundations and algorithms [book review]," *IEEE Comput. Intell. Mag.*, vol. 8, no. 1, pp. 77–79, Feb. 2013, doi: 10.1109/mci.2012.2228600.
[29] Y. Cao, G. Liu, D. Luo, D. P. Bavirisetti, and G. Xiao, "Multi-timescale photovoltaic power forecasting using an improved stacking ensemble algorithm based LSTM-informer model," *Energy*, vol. 283, Nov. 2023, Art. no. 128669, doi: 10.1016/j.energy.2023.128669.
[30] E. Ofori-Ntow, Y. Y. Ziggah, M. J. Rodrigues, and S. Relvas, "A new long-term photovoltaic power forecasting model based on stacking generalization methodology," *Natural Resour. Res.*, vol. 31, no. 3, pp. 1265–1287, Apr. 2022, doi: 10.1007/s11053-022-10058-3.
[31] W. Khan, S. Walker, and W. Zeiler, "Improved solar photovoltaic energy generation forecast using deep learning-based ensemble stacking approach," *Energy*, vol. 240, Feb. 2022, Art. no. 122812, doi: 10.1016/j.energy.2021.122812.
[32] D. F. Specht, "A general regression neural network," *IEEE Trans. Neural Netw.*, vol. 2, no. 6, pp. 568–576, Nov. 1991, doi: 10.1109/72.97934.
[33] M. Hossain, S. Mekhilef, M. Danesh, L. Olatomiwa, and S. Shamshirband, "Application of extreme learning machine for short term output power forecasting of three grid-connected PV systems," *J. Cleaner Prod.*, vol. 167, pp. 395–405, Nov. 2017, doi: 10.1016/j.jclepro.2017.08.081.
[34] Y. Cheng, W. Qi, and W.-Y. Cai, "Dynamic properties of Elman and modified Elman neural network," in *Proc. Int. Conf. Mach. Learn. Cybern.*, Nov. 2002, pp. 637–640, doi: 10.1109/ICMLC.2002.1174413.
[35] *UO Solar Radiation Monitoring Laboratory*. Accessed: Jun. 1, 2023. [Online]. Available: http://solardat.uoregon.edu/index.html
[36] Weather Underground. (2019). *Weather Forecast & Reports—Long Range & Local*. [Online]. Available: https://www.wunderground.com/
[37] F. Wang, Z. Zhang, C. Liu, Y. Yu, S. Pang, N. Duić, M. Shafie-Khah, and J. P. S. Catalão, "Generative adversarial networks and convolutional neural networks based weather classification model for day ahead short-term photovoltaic power forecasting," *Energy Convers. Manage.*, vol. 181, pp. 443–462, Feb. 2019, doi: 10.1016/j.enconman.2018.11.074.
[38] A. Mellit and A. M. Pavan, "A 24-h forecast of solar irradiance using artificial neural network: Application for performance prediction of a grid-connected PV plant at Trieste, Italy," *Sol. Energy*, vol. 84, no. 5, pp. 807–821, May 2010, doi: 10.1016/j.solener.2010.02.006.

LUYAO LIU received the B.E. and Ph.D. degrees from Shandong University, in 2016 and 2022, respectively. She is currently a Postdoctoral Researcher with China Energy Engineering Group Guangdong Electric Power Design Institute Company Ltd. She is also a Research Associate with the Shenzhen International Graduate School, Tsinghua University. Her research interests include load and renewable power forecast and integrated energy system coordinated optimization.

QIE SUN received the Ph.D. degree from the Royal Institute of Technology, in 2011. He is currently a Professor with the Institute for Advanced Science and Technology, Shandong University. His research interests include sustainable energy systems and advanced energy storage.

RONALD WENNERSTEN is currently a Professor with the Institute for Advanced Science and Technology, Shandong University. His current research interests include energy transition and energy technology development.

ZHIGANG CHEN, photograph and biography not available at the time of publication.